Influences of annealing heat treatment on phase structure and electrochemical properties of Zr(MnVNi)$_2$ hydrogen storage alloys

W.K Zhang[a,*], C.A. Ma[a], X.G. Yang[b], Y.Q. Lei[b], Q.D. Wang[b], G.L. Lu[c]

[a]*Department of Applied Chemistry, Zhejiang University of Technology, Hangzhou 310014, PR China*
[b]*Department of Materials Science and Engineering, Zhejiang University, Hangzhou 310027, PR China*
[c]*Central Laboratory, Zhejiang University, Hangzhou 310028, PR China*

Abstract

The influences of annealing treatment on the phase structure and the electrochemical properties of Zr(Mn$_{0.25}$V$_{0.20}$Ni$_{0.55}$)$_2$ and Zr(Mn$_{0.05}$V$_{0.40}$Ni$_{0.55}$)$_2$ hydrogen storage alloys were investigated by means of XRD analysis and electrochemical tests. As-cast alloys were comprised of Laves phases (i.e., C15 and C14) dispersed Zr–Ni phases (Zr$_9$Ni$_{11}$ and ZrNi) and exhibited good overall electrochemical properties. When the as-cast alloys were annealed, the Zr–Ni phases and part of C14 phase decomposed completely with increasing annealing time. The thermodynamically stable phase structure of the annealed alloys was a mixture of C15 and C14 Laves phase. The decomposition of Zr–Ni phases and part of C14 phase resulted in a remarkable decrease in capacity and activation property as compared to those of the as-cast alloy. A synergistic effect due to the presence of Zr–Ni phases in the Laves phases is inferred. The deterioration in the overall electrochemical properties is attributed to the decomposition of the Zr–Ni phases. © 1999 Published by Elsevier Science S.A. All rights reserved.

Keywords: Annealing treatment; Phase structure; Electrochemical properties; AB$_2$-type Zr-based hydrogen storage alloys

1. Introduction

The main advantages of AB$_2$-type Zr-based Laves phase hydrogen storage alloys used as an electrode material compared with the AB$_5$-type alloys are as follows: (1) its higher capacity (e.g., 350–400 mAh/g) in comparison with 250–300 mAh/g of the AB$_5$-type alloys; (2) its longer lifetime (>500 cycles) [1,2]. In recent years, interest in the development of Zr-based Laves phase alloys has considerably increased due to their advantages, and its potential as a promising candidate for AB$_5$-type alloys in large Ni–MH batteries.

Unlike the common AB$_5$-type hydrogen storage alloys, AB$_2$ type Zr-based hydrogen storage alloys commonly are of multiphase structure. Besides the major Laves phases such as C15 and C14 phase, some minor Zr–Ni phases in the forms of Zr$_9$Ni$_{11}$, Zr$_7$Ni$_{10}$ are also present in the alloys [3,4]. As many as five phases were reported for some hydrogen storage alloys by Ovshinsky and his coworkers [5] who proposed that the electrochemical activity of the major phase existed in Zr-based alloys was improved due to the presence of the minor phases. And an improvement in electrochemical properties of Zr-based hydrogen storage alloys was thus obtained.

It is well-known that the phase composition of Zr-based hydrogen storage alloys would change by annealing heat treatment. However, the effects of annealing on the electrochemical properties have not been clarified yet. Moriwaki et al. [6] found that the phase composition of ZrMn$_{0.6}$Cr$_{0.2}$Ni$_{1.2}$ alloy was homogenized after the annealing treatment, and the hydrogen absorbing property and electrochemical properties were both improved. Sawa et al. [7] also reported that the Zr-based hydrogen storage alloys in a single Laves phase structure exhibited better electrochemical properties. However, on the contrary, some authors obtained entirely different results [8,9]. The study of Yu et al. [8] disclosed that the as-cast ZrMn$_{0.6}$Cr$_{0.25}$V$_{0.05}$Ni$_{1.3}$ alloy was still composed of the major phases (i.e., Laves phases C14 and C15) and the minor phases (Zr–Ni phases, such as Zr$_7$Ni$_{10}$ and Zr$_9$Ni$_{11}$). The C14 and Zr$_9$Ni$_{10}$ phases decomposed during annealing, and the phase composition was simplified gradually. However, the discharge capacity of the annealed alloy without Zr$_7$Ni$_{10}$ phase was reported to be much lesser as compared with the as-cast ones. McCormack et al. [9] also found a similar result for Zr–Cr–Ni hydrogen storage alloy that the as-cast Zr–Cr–Ni alloys consisted of

---

Laves phases and Zr–Ni phases and after annealing treatment, the Zr–Ni phase in alloys disappeared. According to his report, the electrochemical capacity and activity of annealed Zr–Cr–Ni alloys all declined owing to the disappearance of Zr–Ni phases. In our previous work [10], $Zr(Mn_{0.45-x}V_xNi_{0.55})_2$ ($x=0.0–0.40$) alloys were found to exhibit an good overall electrochemical property in the range of $x=0.05–0.25$. At $x=0.20$, the alloy gave a maximum capacity of 342 mAh/g at the discharge current of 50 mA/g. With the increasing of the V content, the overall electrochemical property declined gradually and the discharge capacity decreased to 246 mAh/g at $x=0.40$. However, at $x=0.20$ or 0.40, the alloys had the similar phase composition.

In this work, $Zr(Mn_{0.25}V_{0.20}Ni_{0.55})_2$ and $Zr(Mn_{0.05}V_{0.40}Ni_{0.55})_2$ alloys were first cast and annealed at 1080°C for 4 h and 8 h respectively and then the phase structure and electrochemical properties were investigated to clarify the contradictory results in the literature.

2. Experimental details

The alloys $Zr(Mn_{0.25}V_{0.20}Ni_{0.55})_2$ and $Zr(Mn_{0.05}V_{0.40}Ni_{0.55})_2$ were prepared by mixing appropriate amounts of constituent elements, the purity of which was above 99.9% and melting in an arc button furnace under argon atmosphere. All ingots were turned over and remelted three times to ensure homogeneity.

A part of each as-cast ingot was put into a quartz tube, evacuated to 10^{-3} torr, then sealed and annealed in a furnace at 1080°C for 4 and 8 h, respectively.

The as-cast and the annealed alloy samples were crushed mechanically in air to pass through 300-mesh sieve for XRD analysis and electrochemical tests. X-ray diffraction studies were performed by a Rigaku D/Max IIIB diffractometer with Cu Kα radiation.

The preparation of metal hydride electrodes and their electrochemical performance tests were carried out according to the procedures in a previous paper [11].

3. Results and discussion

3.1. Phase analysis

Fig. 1 shows the XRD patterns of the as-cast and annealed $Zr(Mn_{0.25}V_{0.20}Ni_{0.55})_2$ and $Zr(Mn_{0.05}V_{0.40}Ni_{0.55})_2$ alloys. As shown in Fig. 1, the major phases occurred in as-cast alloys are Laves phases, involving f.c.c C15 and hex. C14 with some coexisting minor Zr–Ni phases Zr_9Ni_{11} and ZrNi. After 4 h annealing treatment, most of Zr_9Ni_{11} and all the ZrNi phase are decomposed. The intensity of diffraction peak of C14 phase decreases slightly and that of C15 phase strengthens, indicating that the abundance of C15 phase is increased and that of C14

phase decreased. When the duration of annealing increases to 8 h, only C15 and C14 phase co-exist in alloys, with no evidence of the existence of Zr–Ni phases, indicating the complete decomposition of Zr–Ni phase after 8 h annealing. The results imply that C15 phase is the most thermodynamically stable and C14 phase comes the second. On the contrary, Zr–Ni phases are the least stable ones.

According to the XRD patterns, the main diffraction peaks for C15 or C14 phase become sharper after annealing treatment, indicating that the homogeneity and crystallinity of the annealed alloys are improved.

Fig. 2 illustrates the optical micrograph of $Zr(Mn_{0.25}V_{0.20}Ni_{0.55})_2$ alloy. For the as-cast sample, the alloy contains three different regions, the white (region A), the grey (region B) and the black (region C). The SEM and EDX analysis showed that in the region A (located inside region B) Zr and Ni element exist mainly corresponding to the Zr–Ni phase, with small amount of V and Mn element distributing uniformly in it. The region B and C corresponded to C15 and C14 Laves phases respectively. The result is in good agreement with that of XRD analysis. For 4 h and 8 h annealed alloys, there only exist two regions, the white (region A) and the black (region B) corresponding to C15 and C14 phases, agreeing well with the results of XRD analyses. SEM and EDX analyses display that the elements in the above two regions are approximately of the stoichiometric ratio, suggesting that the annealing treatment leads to the homogenization of the phase composition.

The results of XRD analyses are summarized in Table 1. The lattice parameters as well as the volume of the unit cell of C15 are increasing with the increase in annealing time. However, for the C14 phase, the lattice parameters in the a-axis and the c-axis directions are decreasing with the increase in the annealed time. As a result, the volume of unit cell of the C14 phase is reduced. The changes in lattice parameters indicate also that homogenization phenomenon has taken place during the annealing treatment.

3.2. Electrochemical properties

Fig. 3 shows the electrochemical activation properties of the as-cast and annealed alloys. As shown in Fig. 3, the as-cast $Zr(Mn_{0.25}V_{0.20}Ni_{0.55})_2$ and $Zr(Mn_{0.25}V_{0.20}Ni_{0.55})_2$ alloys have activated fully after 30–40 cycles. However, for the annealed alloys, the capacities still increase after 70 cycles and the charging–discharging cycle numbers for activating increase with the increase of annealing time, indicating that the activation property of the annealed alloys decreases. The electrochemical discharge capacity also decreases markedly with the increase of the annealing time. For example, the highest discharge capacity is 342 mAh/g for the as-cast $Zr(Mn_{0.25}V_{0.20}Ni_{0.55})_2$ alloy, and the discharge capacity reduced to 226 mAh/g and 163 mAh/g after 4 and 8 h annealing treatment respectively. For the annealed alloys the activation process could be
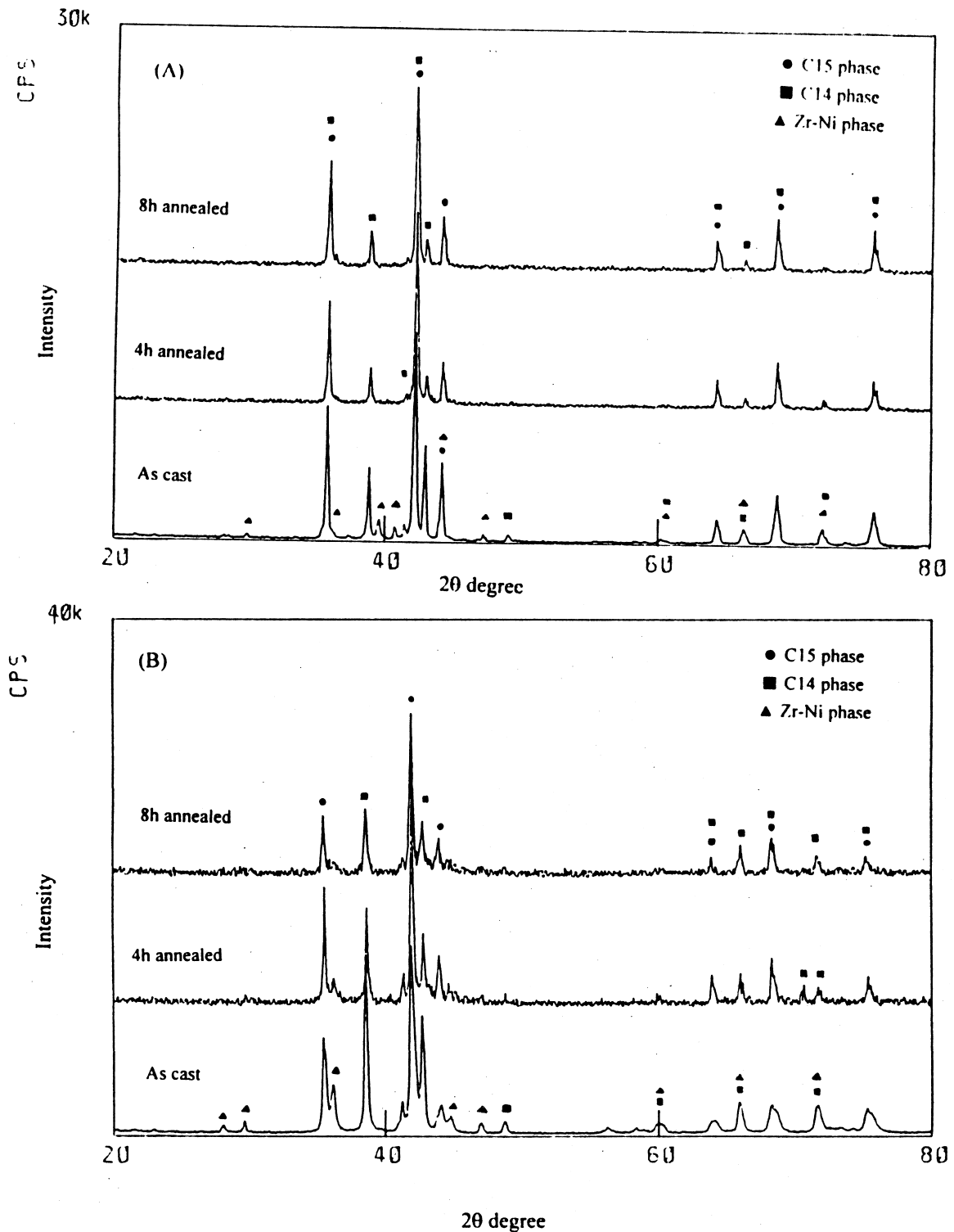
Fig. 1. XRD patterns of the as-cast and annealed alloys. (A) $Zr(Mn_{0.25}V_{0.20}Ni_{0.55})_2$; (B) $Zr(Mn_{0.05}V_{0.40}Ni_{0.55})_2$.

regarded to almost complete after 70 cycles. The longer the annealing time, the larger the decrease in discharge capacity. For $Zr(Mn_{0.05}V_{0.40}Ni_{0.55})_2$ alloy, a similar tendency occurs.

Fig. 4 depicts the linear polarization curves of $Zr(MnVNi)_2$ alloy electrodes in their full-charged state. As

shown in Fig. 4, the slopes of the polarization curves increase with the increase in annealing time, indicating that the exchange current decreases with the increasing annealing time. The values of the exchange current could be calculated according to Butler–Volmer equation.

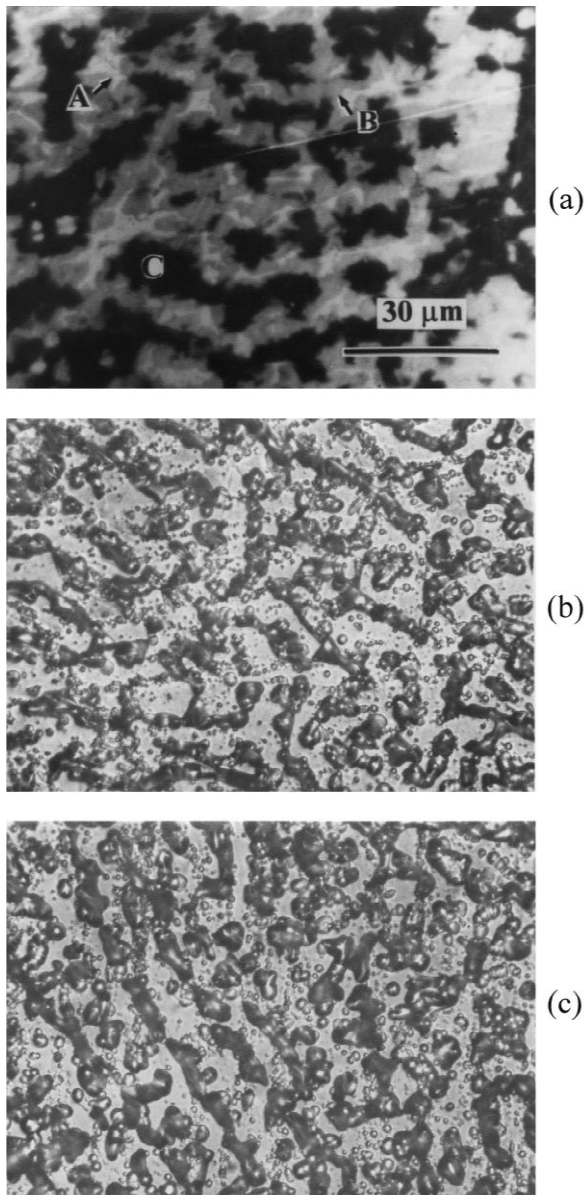The discharge capacity, high-rate dischargeability as

Fig. 2. Optical micrograph of $Zr(Mn_{0.25}V_{0.20}Ni_{0.55})_2$.(A) As-cast; (B) 4 h annealed; (C) 8 h annealed.

well as exchange current of the above alloys are summarized in Table 2. With the increasing annealing time, the high-rate dischargeability, discharge capacity as well as the exchange current all decrease gradually compared to those of the as-cast alloys. This indicates that the annealing treatment deteriorates the electrochemical performances.

3.3. Discussion

In previous studies, some authors [12] have found that some Zr–Ni alloy phases can absorb a large quantity of hydrogen. The hydrogen absorbed by ZrNi, Zr_9Ni_{11} and Zr_7Ni_{10} phase amounts to 460 mAh/g, 340 mAh/g and 370 mAh/g respectively. Unfortunately, the hydrides of these alloys are too stable to desorb their hydrogen at room temperatures, i.e., the absorbing–desorbing hydrogen plateau pressures are too low to desorb the absorbed hydrogen. As a result, the reversible electrochemical capacities of these alloys are also rather low. However, the activation property of these Zr–Ni phases has been found to be very good and the degradation rates of their electrochemical capacity very slow [12]. This indicates that the Zr–Ni alloy phase can offer a surface with good catalytic activity and corrosion-resistance. Joubert et al. [13] reported the Laves phases and Zr–Ni phases to have a synergistic effect on the electrochemical properties of Zr–Cr–Ni alloys. The precipitation of Zr–Ni phases in Zr–Cr–Ni alloys improves the electrochemical properties of Zr–Cr–Ni alloys considerably. Notten et al. [14] also found that the electrochemical properties of AB_5-based hydrogen storage alloys were improved significantly in the presence of a minor secondary alloy phase with higher electrocatalytic activity, i.e., a synergistic effect existed between the major phase and the minor residual phase.

In this study, it is found that the overall electrochemical properties are dependent upon the existence of the Zr–Ni phases in $Zr(MnVNi)_2$ alloys. The as-cast alloys containing Zr–Ni phases exhibit better overall electrochemical properties. However, after annealing treatment, the Zr–Ni phases gradually decompose with the increase of the annealing time, leading to a significant electrochemical

Table 1
Changes in lattice parameters of C15 and C14 Laves phases before and after annealing treatment

| Alloy composition	Main component phases	Lattice parameters (Å)
$Zr(Mn_{0.25}V_{0.20}Ni_{0.55})_2$		
As-cast samples	(1) C15; (2) C14	(1) $a=7.0831$; (2) $a=5.0200$; $c=8.1989$
4 h annealed	(1) C15; (2) C14	(1) $a=7.0983$; (2) $a=5.0187$; $c=8.1973$
8 h annealed	(1) C15; (2) C14	(1) $a=7.0942$; (2) $a=5.0148$; $c=8.1902$
$Zr(Mn_{0.05}V_{0.40}Ni_{0.55})_2$		
As-cast	(1) C15; (2) C14	(1) $a=7.0106$; (2) $a=5.0482$; $c=8.2542$
4 h annealed	(1) C15; (2) C14	(1) $a=7.1282$; (2) $a=5.0393$; $c=8.2453$
8 h annealed	(1) C15; (2) C14	(1) $a=7.1294$; (2) $a=5.0374$; $c=8.2416$
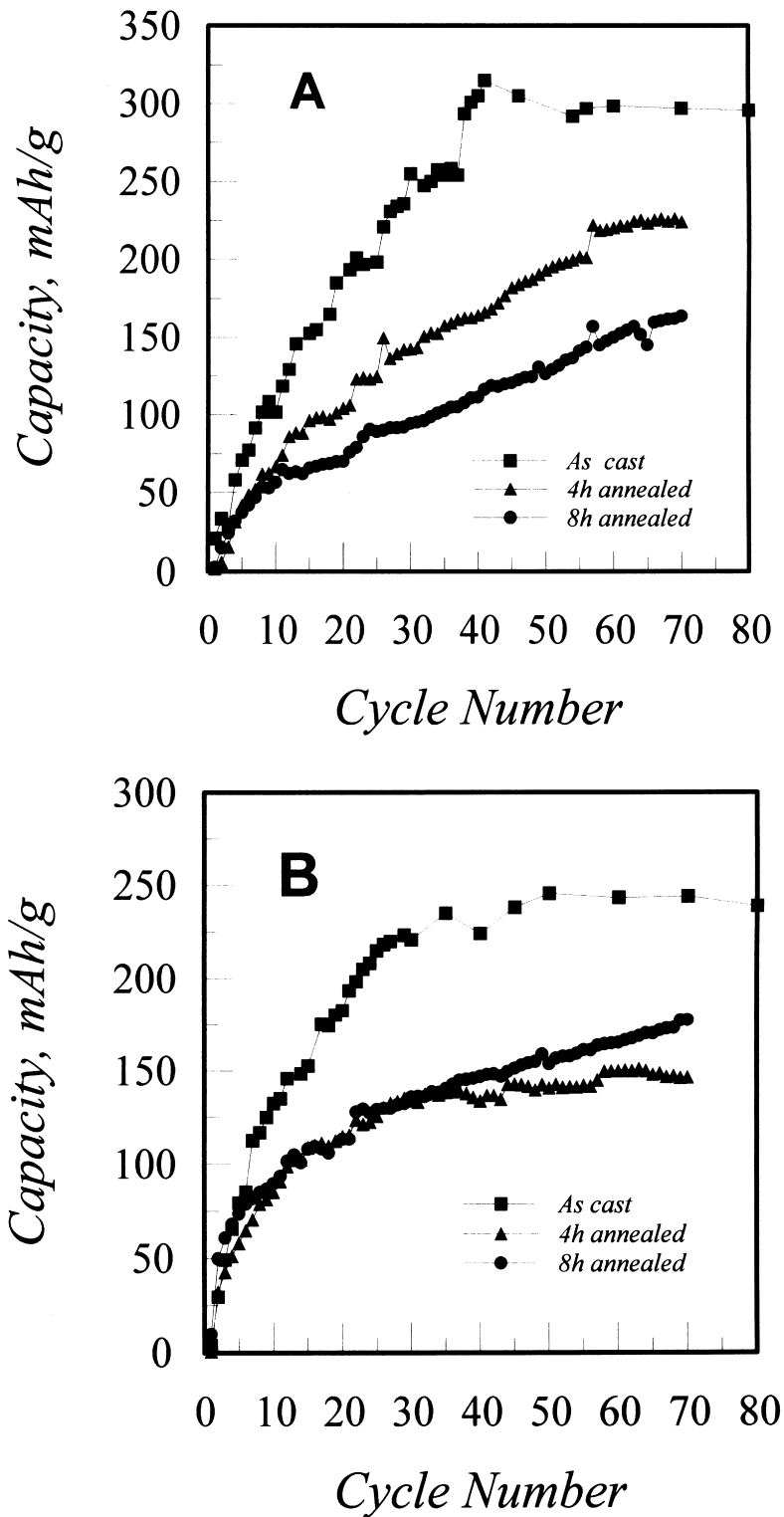
Fig. 3. Activation curves of $Zr(MnVNi)_2$ alloys before and after annealing treatment. (A) $Zr(Mn_{0.25}V_{0.20}Ni_{0.55})_2$; (B) $Zr(Mn_{0.05}V_{0.40}Ni_{0.55})_2$.

performances deterioration. In this experiment, after 4 h annealing treatment, some residual Zr_9Ni_{11} phase still exists, but after 8 h annealing treatment, the Zr–Ni phases decomposed completely. The electrochemical properties of the alloys after 4 h annealing treatment is also better than those of alloys annealed for 8 h. The results also prove that a synergistic effect exists between the Zr–Ni phases and the Laves phases. Therefore, the decrease of the overall electrochemical properties of the annealed alloys should be attributed to the disappearance of Zr–Ni phases in
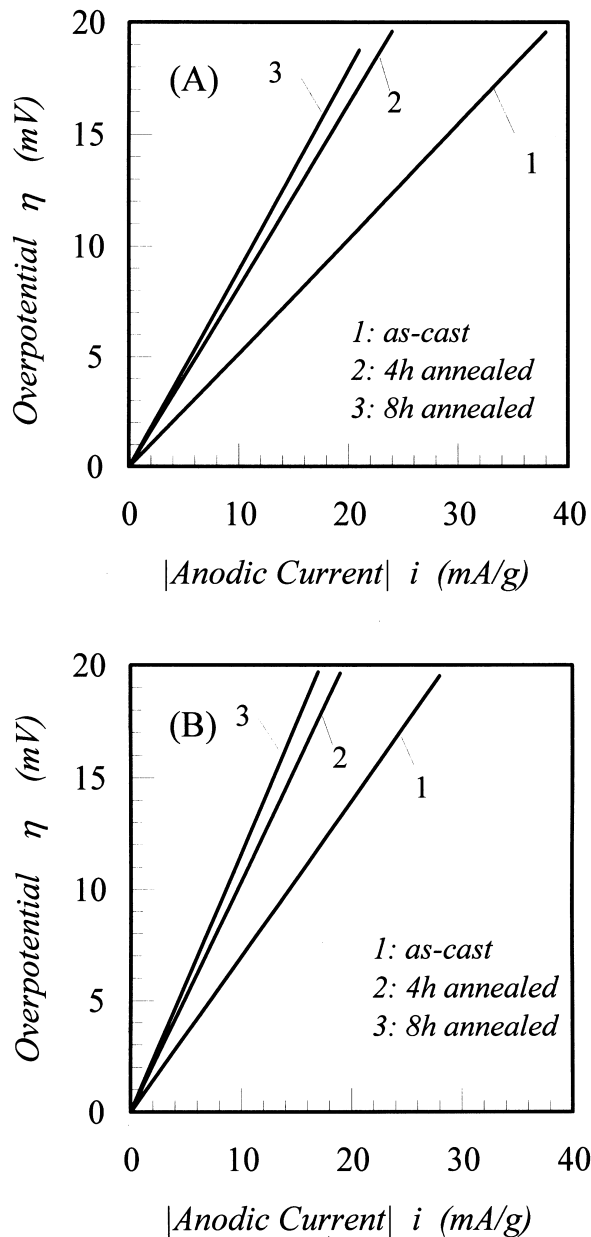
Fig. 4. The linear polarization curves of Zr(MnVNi)$_2$ alloy electrodes. (A) Zr(Mn$_{0.25}$V$_{0.20}$Ni$_{0.55}$)$_2$, equilibrium potential: As cast -0.9478 V; 4 h annealed: -0.9442 V; 8 h annealed -0.9421V. (B) Zr(Mn$_{0.05}$V$_{0.04}$Ni$_{0.55}$)$_2$, equilibrium potential: As cast -0.9465V; 4h annealed -0.9432V; 8h annealed -0.9405V. Scan rate: 5 mV/s.

Zr(MnVNi)$_2$ alloys. Further works on the function of the ZrNi phases are in progress to order to clarify the detailed mechanisms.

4. Conclusions

In this work, the influences of annealing treatment on the phase structure and electrochemical properties of Zr(MnVNi)$_2$ alloys was studied. The conclusions are as follows:

1. The as-cast Zr(Mn$_{0.25}$V$_{0.20}$Ni$_{0.55}$)$_2$ and Zr(Mn$_{0.05}$V$_{0.40}$Ni$_{0.55}$)$_2$ alloys both contain Laves phases and Zr–Ni phases. With the increasing of the annealing time, the Zr–Ni phases disappear gradually and part of the C14 phase transforms into C15 phase. As a result, the final stable phase structure of the alloys is a mixture of C15 and C14 Laves phase. The phase composition is also homogenized.
2. After the annealing treatment, the overall electrochemical properties decrease significantly with the decomposition of the Zr–Ni phases. This indicates that the annealing treatment is harmful to the electrochemical performances.
3. A synergistic effect between the Laves phase and the Zr–Ni phases is thus inferred in Zr (MnVNi)$_2$ alloys. The deterioration of the overall electrochemical properties is ascribed to the disappearance of the Zr–Ni phases in alloys.

Acknowledgements

References

[1] H. Nakano, S. Wakao, J. Alloys Comp. 231 (1995) 1587–1593.
[2] X.G. Yang, Y.Q. Lei, W.K. Zhang, G.M. Zhu, Q.D. Wang, J. Alloys Comp. 243 (1996) 151–155.

Table 2
High rate-dischargeability and exchange current i^0 for as-cast and annealed alloys

Alloy composition	Discharge capacity (mAh/g)	High-rate dischargeability $C_{200}/(C_{200}+C_{50})$, %	Exchange current i^0, (mA/g)
Zr(Mn$_{0.25}$V$_{0.20}$Ni$_{0.55}$)$_2$ alloy			Full-charged state:
As-cast	342	75.1	49.9
1080°C×4 h	226	68.5	32.4
1080°C×8 h	163	63.2	29.6
Zr(Mn$_{0.05}$V$_{0.40}$Ni$_{0.55}$)$_2$ alloy			Full-charged state:
As-cast	245	52.7	38.2
1080°C×4 h	177	50.2	25.1
1080°C×8 h	150	45.7	22.4

[3] S. Wakao, H. Sawa, J. Less-Common Met. 172–174 (1991) 1219–1226.

[4] Y. Moriwaki, T. Gamo, T. Iwaki, J. Less-Common Met. 172–174 (1991) 1028.

[5] S.R. Ovshinsky, M.A. Fetcenko, J. Ross, Science 260 (1993) 176–181.

[6] Y. Moriwaki, T. Gamo, H. Seri, T. Iwaki, J. Less-Common Met. 172–174 (1991) 1211.

[7] H. Sawa, S. Wakao, Mater. Tran., JIM 31 (1990) 487–492.

[8] J.Y. Yu, Ph.D dissertation of Zhejiang University, 1995

[9] M. MaCormack, M.E. Badding, G. Vyas, S.M. Zahurak, D.W. Murphy, J. Electrochem. Soc. 143 (2) (1996) L31–L33.

[10] W.K. Zhang, Y.Q. Lei, X.G. Yang, Q.D. Wang, Trans. Non-ferrous Met. Soc. China (in Chinese) 7 (3) (1996) 72–76.

[11] W.K. Zhang, Y.Q. Lei, X.G. Yang, Q.D. Wang, Trans. Non-ferrous Met. Soc. China, 7 (3) (1998) 72–76.

[12] J.-M. Joubert, M. Latroche, A. Percheron-Guegan, J. Alloys Comp. 231 (1995) 494.

[13] J.M. Joubert, M. Latroche, A. Percheron-Guegan, J. Bouet, J. Alloys Comp. 243 (1996) 219–228.

[14] P.H.L. Notton, P. Hokkeling, J. Electrochem. Soc. 138 (7) (1991) 1877–1885.